Journal of Magnetism and Magnetic Materials 394 (2015) 96–104

Contents lists available at ScienceDirect

Journal of Magnetism and Magnetic Materials

journal homepage: www.elsevier.com/locate/jmmm

Electrical and morphological properties of magnetocaloric nano ZnNi ferrite

O.M. Hemeda [a,*], Nasser Y. Mostafa [b,c], Omar H. Abd Elkader [d,e], D.M. Hemeda [a], A. Tawfik [a], M. Mostafa [a]

[a] Physics Department, Faculty of Science, Tanta University, Tanta, Egypt
[b] Materials and Corrosion Group, Department of Chemistry, Faculty of Science, Taif University, Saudi Arabia
[c] Chemistry Department, Faculty of Science, Suez Canal University, Ismailia 41522, Egypt
[d] Electron Microscope & Thin Films Department, Physics Division, National Research Center, Dokki 12622, Cairo, Egypt
[e] Electron Microscope Unit, Zoology Department, College of Science, King Saud University, Riyadh, Saudi Arabia

ARTICLE INFO

Article history:
Received 24 March 2015
Received in revised form
6 May 2015
Accepted 21 May 2015
Available online 17 June 2015

Keywords:
Nano ZnNi ferrite
combustion technique
Electrical and morphological properties
Magnetic entropy
HRTEM

ABSTRACT

A series of $Zn_{1-x}Ni_xFe_2O_4$ nano ferrite (with $x=0$, 0.2, 0.4, 0.6, 0.8, and 1) compositions were synthesized using the combustion technique. The powder samples were characterized by XRD. The X-ray analysis showed that the samples were single phase spinel cubic structure. The AC resistivity decreases by increasing the frequency from 1 kHz to 10 kHz. As the frequency of the applied field increases the hopping of charge carrier also increase, thereby decreasing the resistivity. A shift in dielectric maximum is observed toward higher temperature with increasing the Ni content from 536 K to 560 K at 1 kHz. The HRTEM (high resolution TEM) images of four compositions have lattice spacing which confirms the crystalline nature of the samples. The surface morphology SEM of the sample consists of some grains with relatively homogenies distribution with an average size varying from 0.85 to 0.92 µm. The values for entropy change in this work are still small but are significally higher than the values that have been reported for iron oxide nanoparticle. The magnetic entropy change was calculated from measurements of $M\ (H, T)$ where H is the magnetic field and T is the temperature. The maximum value of entropy change (ΔS) obtained near Curie temperature which makes these material candidates for magnetocaloric applications.

1. Introduction

The magnetocaloric effect (MCE) is definned as the heating or cooling (i.e., the temperature change) of a magnetic material due to the application of a magnetic field. This effect has been called adiabatic demagnetization for years, though this fenomenon is one practical application of the MCE in magnetic materials. For excellent reviews on the magnetocaloric effect, see references [1,2]. The magnetocaloric effect was discovered in 1881, when Warburg observed it in iron [3]. The origin of the MCE was explained independently by Debye [4] and Giauque [5]. They also suggested the first practical use of the MCE: the adiabatic demagnetization, used to reach temperatures lower than that of liquid helium, which had been the lowest achievable experimental temperature. Nowadays, there is a great deal of interest in using the MCE as an alternative technology for refrigeration, from room temperature to the temperatures of hydrogen and helium liquefaction (300–4.2 K). The magnetic refrigeration offers the prospect of an energy-efficient and environtment friendly alternative to the common vapor-cycle refrigeration technology in use today [6,7].

Magnetic refrigeration is rapidly becoming competitive with conventional gas compression technology because it offers considerable operating cost savings, mechanical stability, light weight and better performance [8]. For many years magnetocaloric effect (MCE) has been successfully used to reach ultra-low temperatures in a research environment. $Gd_5Si_{1.5}Ge_{2.5}$ is the best known example of a material that exhibits giant MCE [9]. Additionally, most of the current bulk MCE materials rely on the entropy change associated with the paramagnetic–ferromagnetic transition at the Curie temperature. The MCE shows a maximum around the Curie temperature and drops rapidly on either side [10]. It has been theoretically shown that by reducing the average particle size close to the single magnetic domain, magnetic entropy change increases by several orders of magnitude as compared to the entropy change in bulk materials [11]. In addition, the large surface

---

* Corresponding author.
E-mail address: omhemeda@yahoo.co.uk (O.M. Hemeda).

http://dx.doi.org/10.1016/j.jmmm.2015.05.059
0304-8853/

area in nanostructured materials has the potential to provide better heat exchange with the surrounding materials.

The MCE can be measured directly or can be calculated via different methods using the field dependent specific heat values [12]. Also, the MCE can be calculated from magnetization (M) measurements, through a thermodynamic Maxwell equation, which can be derived from the first law of thermodynamics [13]

$$\left(\frac{\partial S}{\partial H}\right)_T = \left(\frac{\partial M}{\partial T}\right)_H$$

In this paper, we have presented our results on the entropy change in Ni and zinc ferrite nanoparticles. The present work is mainly focused on the morphological and electrical properties of ferrite. The effect of Ni on MCE and resistivity is analyzed. The aim of the present work is to study the electrical and magnetic properties of $Zn_{1-x}Ni_x\ Fe_2O_4$ nanoparticles prepared by solution combustion method, and to indicate its ability as magnetocaloric material.

2. Materials and methods

Nanoparticles of cobalt ferrite were prepared by solution combustion method. Analytical grade nickel nitrate ($Ni(NO_3)_2\cdot 6H_2O$), zinc nitrate ($Zn(NO_3)_2\cdot 6H_2O$) and ferric nitrate ($Fe(NO_3)_3\cdot 9H_2O$) was taken as oxidants while glycine (CH_2NH_2COOH) (98%) was employed as fuel to drive the combustion reaction. According to propellant chemistry, the total oxidizing valences the metal nitrates should be balanced by total reducing valences of fuel in order to release maximum energy. A stoichiometric mixture of fuel and oxidant is one in which the quantity of oxidant present is theoretically correct for complete oxidation. The combustion reactions can be represented as follows:

$$M(NO_3)_2 + 2Fe\ (NO_3)_3 + z\ NH_5C_2O_2\ (aq) \rightarrow MFe_2O_4\ (s) + z\ CO_2(g) + (5+z)N_2(g) + (9+2\ z)\ H_2O(g)$$

Where, M=Zn and/or Ni and $\boldsymbol{z}=4.555$, is the multiplication factor in order to get fuel lean ($\phi=1$). In case $\phi=1$ represents the stoichiometric condition at which oxygen content of oxidizer can be reacted to consume fuel entirely [14].

In typical procedure, the stoichiometric amounts of cobalt nitrate, ferric nitrate and glycine (1:2:4.555 M ratios) were taken in a glass beaker. A minimum amount of distilled water was added with stirring to completely dissolve all constituents. The beaker was then kept on furnace preheated to 400 °C. The whole combustion reaction process was complete in less than 5 min whereas actual time of ignition was less than 5 s. the remaining fluffy product was collected from the beaker. This synthesis route needs no subsequent heat step.

X-ray diffraction patterns (XRD) were obtained using Bruker diffractometer D8-advance with Cu-K_α radiation. Determination of the lattice constants were made by least squares refinement of the X-ray diffraction data. Indexing of the powder patterns and least squares fitting of the unit cell parameters was possible using the software X'Pert HighScore Plus [15]. The powders morphology was investigated using SEM (JOEL, Model: JSM-5600, Japan.) equipped with secondary electron detector and EDX. All samples were coated with gold. The high resolution transmission electron microscope was performed using Jeol -2100 HRTM in NRC. RLC Bridge of type BM 591 was used for the measurement the dielectric constant ($\acute{\varepsilon}$), dielectric loss ($\tan\delta$), AC resistivity and magnetic permeability (μ_i) for all toroidal samples at 1 kHz and different temperature. The temperature of the sample was measured by Ni Cr–Ni thermocouple. The measurements were carried from room temperature up to 825 K. The magnetization as a function of temperature and magnetic field has been measured in the previous work using Faraday method [16]. The entropy changes were calculated from magnetization crves using Maxwell's equation.

3. Result and discussions

3.1. structral analysis

The x-ray diffraction patterns for the nano ferrite $Zn_{1-x}Ni_xFe_2O_4$ synthesized by solution combustion technique are shown in Fig. 1. The existence of (111) (220) (311) (222) (400) (422) (511) and (440) major lattice planes in the XRD patterns confirms the formation of a single phase spinel cubic structure of space group Fd-3 m for all $Ni_{1-x}\ Zn_xFe_2O_4$ samples with x values up to 1.0. The strongest reflection comes from (311) which characterize the spinel structure. A shift occurs of (311) XRD peak to higher angle (2θ) with the increase of Ni content because the sample with higher Ni content has a smaller lattice parameter. These shifts are larger for Ni nano crystal ferrite compared to the same compositions in bulk state.

This means that the present combustion synthesis resulted in complete conversion of reactants to yield ferrite as a single phase without any calcination processes. The cell parameters were obtained from the fitting of x-ray diffraction patterns carried out applying the XPert HighScore Plus program, are given in Fig. 2. Results showed that increasing the Ni content (x) decreases cell parameter. The small changes in the lattice parameters are due to the incorporation of the slightly small Ni ion in place of the Zn ion.

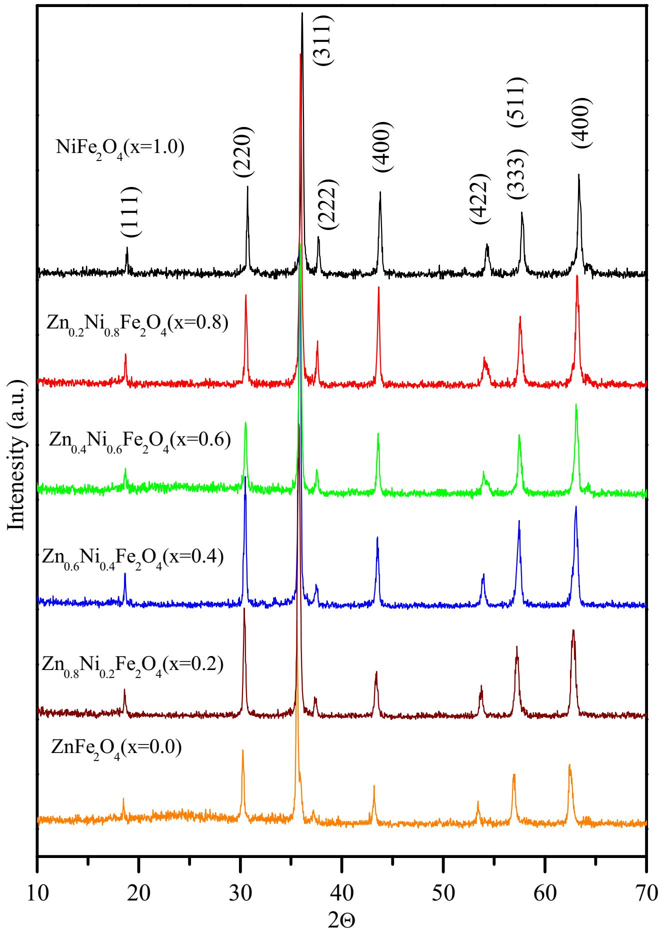

Fig. 1. XRD patterns of the system $Zn_{1-x}Ni_xFe_2O_4$, $x=0.0$, 0.2, 0.4, 0.6, 0.8 and 1.0.